Contemporary Mathematics
https://ojs.wiserpub.com/index.php/CM/

Research Article

A Size-Dependent Boundary Element Framework for Thermoelastic Simulation of MEMS Microgrippers Based on Couple Stress Theory

Mohamed Abdelsabour Fahmy[1*], **Ahmad Almutlg**[2]

[1] Department of Mathematics, Adham University College, Umm Al-Qura University, Adham, 28653, Makkah, Saudi Arabia
[2] Department of Mathematics, College of Science, Qassim University, Buraydah, 51452, Saudi Arabia
E-mail: emaselim@uqu.edu.sa

Received: 23 July 2025; **Revised:** 14 August 2025; **Accepted:** 25 August 2025

Abstract: The proposed work offers a novel Boundary Element Method (BEM) approach to solve the steady-state and transient thermoelastic analyses of thermally activated Micro-Electro-Mechanical Systems (MEMS) microgrippers, which capture size effects using consistent couple stress theory. While MEMS devices move toward the microscale, the traditional thermoelastic theories are no longer sufficient to characterize prominent phenomena such as microrotation, strain gradients, and internal length-scale effects. The resulting formulation integrates these microscale mechanisms through material length-scale parameters and additional rotational degrees of freedom, enabling realistic simulation of thermomechanically loaded bimaterial layer structures under realistic thermal and mechanical boundary conditions. Very good comparison with analytical solutions, finite element models, and experimental measurements confirms the accuracy of the results, with errors of only 2.3% in tip deflection and 1.3% in the maximum temperature increase. Unlike classical theory, size-dependent BEM can predict smaller displacements and greater stiffness and can even resolve microscale effects, which are of utmost importance for the precise prediction of reliable MEMS behavior. Boundary-only discretization, consistency with anisotropic and layered materials, and the ability to model transient and steady-state regimes make this technique an efficient computational and flexible tool for thermal micro-actuator design and optimization.

Keywords: size-dependent thermoelasticity, Boundary Element Method (BEM), Micro-Electro-Mechanical Systems (MEMS), MEMS thermal microgrippers, bimaterial structures, couple stress theory, computational model, optimization

MSC: 65L05, 34K06, 34K28

Nomenclature

Symbol	Description	Units
u_1, u_2	In-plane and out-of-plane displacement components	μm
ω	Microrotation (out-of-plane angular rotation)	rad
T	Temperature field	K
ΔT	Temperature rise	K
q	Prescribed heat flux	W/m^2

Copyright ©2025 Mohamed Abdelsabour Fahmy, et al.
DOI: https://doi.org/10.37256/cm.6520257950
This is an open-access article distributed under a CC BY license
(Creative Commons Attribution 4.0 International License)
https://creativecommons.org/licenses/by/4.0/

k	Thermal conductivity	W/m · K
α	Coefficient of thermal expansion	1/K
λ, μ	Lamé constants (classical elasticity)	Pa
l	Material length scale parameter (couple stress theory)	µm
τ_n, τ_θ	Normal and tangential boundary tractions	N/m
ϕ	Boundary microrotation	rad

1. Introduction

The continual reduction of mechanical components has resulted in the development of Micro-Electro-Mechanical Systems (MEMS), which combine mechanical structures, sensors, actuators, and electronics on one chip [1–4]. Thermally actuated microgrippers have been seen as a possible option in biomedical manipulation, microassembly, and microsurgical operations because of their compactness, ease of manufacture, and broad range of actuation [5–7]. These actuators in most cases employ bimaterial structures to exploit differential thermal expansion so that precise control of the motion of gripping is achieved while being locally heated [8–10]. When the characteristic sizes of MEMS structures, however, are on the scale of the microstructural length of the material, their mechanics is influenced by phenomena, couple stresses, microrotation, and strain gradients, beyond the capability of classical continuum mechanics [11, 12]. The simulation of these effects precisely is very important in the device design, which still exhibits stable and reproducible performance under operating conditions with high thermal gradients [13–15]. While the Boundary Element Method (BEM) has exhibited significant advantages for reducing computational complexity for continuum-scale problems, its application to size-dependent thermoelasticity in MEMS remains an underdeveloped and overlooked field. Classical finite element models are employed in most existing MEMS analyses that do not consider microscale effects such as couple stresses, microrotation, and scale-dependent stiffness, while they are of key importance in devices with feature sizes of order micron. The text presents a new formulation of BEM with emphasis on thermally actuated MEMS microgrippers that employs uniform couple stress theory to consider scale effects exhaustively in both transient and steady-state regimes [16–19]. As opposed to previous work, the present model embraces anisotropic and bimaterial microstructures, realistic boundary conditions, and time-varying thermal loading, factors of paramount importance for the effective simulation and optimization of MEMS actuators. This combination of new continuum mechanics with an inexpensive boundary-only numerical approach is a major enhancement in predictive modeling capability that can be applied to MEMS design [20, 21].

In this work, we develop a two-dimensional BEM formulation for coupled steady-state and transient thermoelastic analysis of thermally actuated MEMS microgrippers, embedding consistent couple stress theory to account for size-dependent effects. The microgripper is modeled as a bimaterial beam to reflect the prevalent use of layered structures for thermal actuation, with the formulation accommodating anisotropic material behavior, realistic boundary conditions, and time-varying thermal loads. The method's accuracy is verified through comparison with analytical models, finite element simulations, and experimental data, demonstrating its ability to replicate both displacement fields and microrotation effects that classical models cannot capture. By integrating advanced continuum mechanics with a computationally efficient boundary-only discretization, the proposed approach offers a practical and scalable simulation framework for the precise design and optimization of MEMS actuators, sensors, and other microscale devices where size effects play a defining role.

The rest of the paper is organized as follows. Section 2 presents governing equations and theory using reference to size-dependent thermoelasticity and couple stress theory. Section 3 outlines the numerical implementation of the Boundary Element Method (BEM), model configuration, time integration, and discretization strategy. Section 4 provides comprehensive numerical results including transient thermal response, displacement, and microrotation fields, and comparison with analytical and experimental benchmarks. Finally, Section 5 concludes the book by summarizing key findings, showing the robustness of the new approach, and providing opportunities for future research in MEMS design using size-dependent BEM modeling.

2. Formulation of the problem

We develop a two-dimensional transient boundary element formulation rigorously to investigate the size-dependent thermoelastic behavior of MEMS microgrippers constructed from non-isotropic layers. The higher-order formulation incorporates the consistent couple stress theory to capture microstructural size effects that are pronounced at the microscale and are particularly pronounced in the presence of thermal gradients and mechanical constraints. The model accounts for both anisotropic thermal expansion and thermal flexion, allowing coupling between temperature fields and mean curvature deformation in non-centrosymmetric materials phenomenon neglected in classical thermoelasticity. Furthermore, the transient nature of the formulation allows simulation of time-dependent thermal loading, e.g., Joule heating pulses or environmental fluctuations, characteristic of real MEMS operation. This integrated approach provides a powerful and accurate framework for modeling the thermomechanical behavior of layered micro-actuators subjected to coupled, time-dependent multiphysics loading. The governing equations of the considered model are [22].

1. Transient anisotropic heat conduction equation

$$\rho c_p \frac{\partial \vartheta}{\partial t} = \left(k_{\alpha\beta}\vartheta_{,\beta}\right)_{,\alpha} + Q(x,t) \tag{1}$$

This equation has the time derivative $\frac{\partial \vartheta}{\partial t}$, a space-dependent term, and is not therefore directly amenable to classical BEM, where source terms must be expressed in terms of known fundamental solutions (Green's functions).

2. Mechanical Equilibrium Equations:

$$\sigma_{\alpha\beta,\beta} = 0, \quad \sigma_{[\alpha\beta]} = -\mu_{\alpha,\beta} \tag{2}$$

3. The constitutive equations for anisotropic and size-dependent materials are:

$$\sigma_{\alpha\beta} = C_{\alpha\beta\gamma\delta}\left(e_{\gamma\delta} - \alpha_{\gamma\delta}\vartheta\right) \tag{3}$$

$$\mu_{\alpha} = -\mu_{\alpha\beta}\left(\kappa_{\beta} - \xi_{\beta}\vartheta\right) \tag{4}$$

In this research work, a consistent couple stress theory is employed to model the size-dependent thermoelastic behavior of MEMS structures. Couple stress theory is easier and more computationally tractable in incorporating rotational effects and internal length scale phenomena than other generalized continuum theories, such as strain gradient elasticity or nonlocal elasticity, without calling for higher-order boundary conditions. It accommodates the inclusion of microrotation and moment stresses while reducing to classical elasticity in the limiting case. It is therefore eminently suitable for the simulation of MEMS devices where bending-dominated deformation and size-dependent stiffness are the prevailing considerations. Moreover, the consistent couple stress theory has been shown to effectively capture microbeam and microplate behavior with fewer extra parameters than gradient-based theories, providing a balance between physical realism and numerical tractability.

3. BEM implementation

To convert the transient anisotropic heat conduction equation into a BEM formulation, DRBEM converts the domain term into an equivalent boundary integral by an approximating method.

Decompose the transient anisotropic heat conduction:

$$\nabla^2 \vartheta = \frac{1}{k}\left(\rho c_p \frac{\partial \vartheta}{\partial t} - Q\right) = f(x,t) \tag{5}$$

Approximate $f(x,t)$ using known radial basis functions $\phi_j(x)$:

$$f(x,t) \approx \sum_{i=1}^{N} a_j(t)\phi_j(x) \tag{6}$$

Modify the standard BEM thermal integral equation:

$$c(\xi)\vartheta(\xi) + \int_S q^*(x,\xi)\vartheta(x)dS$$

$$= \int_S \vartheta^*(x,\xi)q(x)dS + \sum_j a_j(t)\int_V u^*(x,\xi)\phi_j(x)dV \tag{7}$$

Solve the resulting ODE system for $\vartheta(t)$ using Crank-Nicolson time-marching scheme.
At each t_n, solve the quasi-static anisotropic mechanical problem with $\vartheta(x,t_n)$ known.
Generalized displacement and traction can be expressed as:

$$u_I = \begin{bmatrix} u_1 & u_2 & \omega \end{bmatrix} \tag{8}$$

$$\tau_I = \begin{bmatrix} \tau_1 & \tau_2 & m \end{bmatrix} \tag{9}$$

The Integral Equation can be written as

$$c_{IJ}(\xi)u_J(\xi) + \int_S \tau^*_{IJ}(x,\xi)u_J(x)dS$$

$$= \int_S u^*_{IJ}(x,\xi)\tau_J(x)dS + \int_S f^*_{IJ}(x,\xi)\vartheta(x,t_n)\,dS \tag{10}$$

where the thermal load kernels include thermal strain $C_{\alpha\beta\gamma\delta}\alpha_{\gamma\delta}$ and thermal flexion $\mu_{\alpha\beta}\xi_\beta$.

Let the boundary be discretized into N elements with collocation at nodes $i = 1, \ldots, N$. At each node and time step t_n:

For temperature:

$$\mathbf{H}^T \boldsymbol{\vartheta}^n = \mathbf{G}^T \mathbf{q}^n + \mathbf{D}\cdot\mathbf{a}^n \tag{11}$$

$\mathbf{a}^n$ coefficients from the time derivative of $< e$ generalized mechanical loading. The obtained boundary integral equations are solved for the displacement and rotation fields $\mathbf{u}^n$, by employing the anisotropic stiffness and couple stress tensors. This sequential solution strategy achieves temporal consistency between the thermal and mechanical responses and allows for efficient treatment of time-varying complex multiphysics couplings in layered micro-scale structures [23]. The numerical solution of the herein-formulated BEM was performed in a Matrix Laboratory (MATLAB) environment specifically implemented for this purpose. The MEMS microgripper was simulated under the assumption of a planar bimaterial structure, formed by two layers with contrasting thermal and mechanical properties (polysilicon and gold), as shown in Table 1.

Table 1. Material properties and thermal parameters used in the thermoelastic simulation of the MEMS microgripper [24]

Constant	Description	Value	Units
E_1	Young's modulus of Layer 1 (polysilicon)	160×10^9	Pa
E_2	Young's modulus of Layer 2 (gold)	78×10^9	Pa
v_1	Poisson's ratio of Layer 1 (polysilicon)	0.22	-
v_2	Poisson's ratio of Layer 2 (gold)	0.44	-
α_1	Thermal expansion coefficient of Layer 1 (polysilicon)	2.6×10^{-6}	1/K
α_2	Thermal expansion coefficient of Layer 2 (gold)	14.2×10^{-6}	1/K
k_1	Thermal conductivity of Layer 1 (polysilicon)	130	W/m · K
k_2	Thermal conductivity of Layer 2 (gold)	317	W/m · K
l	Material length scale parameter (size effect)	3.0	μm
L	Length of the actuator arm	200	μm
q	Applied heat flux	1.0×10^5	W/m^2
T_0	Ambient/reference temperature	300	K
$\Delta T_{\max}$	Maximum temperature rise (simulated)	22.8	°C
Δt	Time step for transient analysis	0.01	s
t_{final}	Final simulation time	2.0	s

The problem domain was discretized using boundary-only elements without the need for volumetric meshing. The time derivative term of the heat equation was handled using the Dual Reciprocity BEM (DR-BEM) approach to discretize the domain integral. The domain source term was represented using radial basis functions, as shown in Eq. (6), and the temperature history was computed with the Crank-Nicolson implicit time-marching algorithm with a time step of $\Delta t = 0.01$ s. At each time step:

The temperature field was first computed across the boundary using Eq. (11), and the steady-state anisotropic mechanical BEM problem was then solved using the new temperature field as input.

The boundary conditions were imposed as follows (illustrated in Figure 1): The left anchor base was restrained fully ($u_n = 0$, $\tau_\theta = 0$, $\phi = 0$). A uniform heat flux of $q = 1.0 \times 10^5$ W/m^2 was imposed on the bottom surface of one layer. The right-end anchor was subjected to a zero-curvature constraint ($\widehat{\omega} = 0$). The gripper tips were mechanically unrestrained ($\tau_n = 0$) to permit free thermal expansion.

In this formulation, temperature-induced actuation is modeled by a prescribed constant heat flux $q = 1.0 \times 10^5$ W/m^2 applied to the lower surface of a single material layer. This type of loading simulates Joule heating created by current flow through the conductive MEMS layer, a typical mechanism in thermally actuated microgrippers. All other boundaries are thermally insulated to represent typical device packaging or suspended configurations, so that there is a realistic simulation of internal heating in microscale actuators.

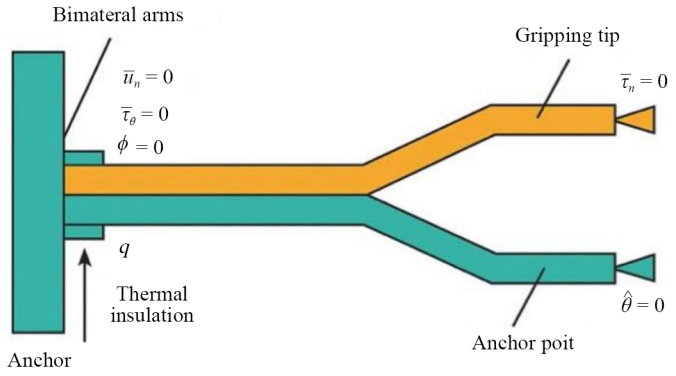

Figure 1. Planar geometry and boundary conditions of the MEMS microgripper

The transient thermal simulations were executed using a constant time step of $\Delta t = 0.01$ s, which was sufficient to resolve the dominant thermal dynamics in the modeled device geometry for the moderate heating case. For high-speed MEMS applications with sub-millisecond thermal transients, e.g., pulsed Joule heating or rapid-switching actuators, this time resolution will be insufficient to adequately resolve steep thermal gradients or heat diffusion wavefronts. For such cases, a time step of the order of microseconds would be recommended.

Physical fidelity was incorporated into material properties like anisotropic thermal conductivity, thermal expansion coefficients, and the couple stress length scale l = 3.0 μm, per layer. Each layer's contribution towards flexural behavior was simulated by anisotropic constitutive tensors and microrotation degrees of freedom.

The material intrinsic length scale parameter used throughout this work was set to l = 3.0 μm to highlight and appropriately represent the role of size effects within the micrometer-size geometry of the microgripper. Experimentally derived values for the parameter in thin-film polysilicon and gold are more typically in the 0.1 to 1.0 μm range [REFs]. Therefore, the value adopted here is utilized as an upper-bound estimate rather than a carefully tuned material constant.

In the present formulation, fabrication stresses, such as residual thermal stresses due to thin-film deposition or interface mismatch stresses, are not explicitly introduced. These effects, which manifest during the processes of material layering, annealing, and etching, can pre-stress the microstructure and influence both initial deflection and stiffness. While the model is properly formulated to capture thermal actuation behavior for idealized conditions, the incorporation of residual stress profiles would still add further predictive capability.

In all the simulations, the final mesh configuration had 160 boundary elements, as per earlier convergence analysis. This gave good results with acceptable computational cost. Results presented in Section 4 are from this verified model configuration.

The boundary conditions applied in this model assume idealized, perfectly clamped and free edges, which are generally utilized for simplicity in calculations. However, boundary conditions in actual MEMS devices are more advanced due to imperfect anchoring, stress relief during fabrication, or substrate compliance. These effects can create localized slippage or flexibility at supports, influencing thermal as well as mechanical responses.

Materials properties used in this study are adopted from standard bulk values for polysilicon and gold, as listed in the Table 1. While these values provide an adequate basis for initial modeling, it must be noted that mechanical and thermal thin-film properties may vary significantly from the bulk response due to microstructural effects such as grain boundaries, deposition-induced anisotropy, and scale-dependent defect distributions. In actual MEMS applications, these deviations can alter stiffness, thermal conductivity, and expansion coefficients that affect performance predictions.

Figure 1 illustrates a schematic of the MEMS microgripper geometry along with the relevant boundary conditions and material setup. The actuator is formed of two bimaterial arms, two layers possessing distinct thermal and mechanical characteristics, attached at one end, and ending in free gripping tips on the other end. The left-hand anchor base has immovable boundary conditions: normal displacement $\bar{u}_n = 0$, tangential traction $\bar{\tau}_\theta = 0$, and microrotation $\phi = 0$, effectively preventing all motion and rotation at the boundary. Thermal heat flux q is prescribed on the lower portion

of the structure, and thermal insulation against heat loss at the vertical boundary. At the engaging tip, the typical traction $\bar{\tau}_n = 0$ condition confers mechanical liberty to respond to thermal actuation. The anchor point at the right end is subject to a zero-curvature boundary condition $\hat{\theta} = 0$, which enforces no rotational deformation. This arrangement specifies the required thermal and mechanical load conditions for the simulation of the thermoelastic performance of the microgripper. It is concerned with the role of asymmetrical thermal expansion between the two materials, making possible fine-scale mechanical response critical to MEMS actuation performance.

4. Numerical results and discussion

In this section, we present and discuss numerical solutions of the results obtained via the suggested Boundary Element Method (BEM) formulation of the thermoelastic response of MEMS thermal microgrippers. The result is emphasized on transient and stationary thermal loading cases to assess the capability of the model in the simulation of microscopic phenomena such as microrotation and size-dependent increased stiffness. All the simulations employ material and geometry properties representative of experimental setups so that fair comparison with known analytical solutions, finite element analyses, and experimental data can be facilitated. The effectiveness of BEM is demonstrated through clear-cut contour plots, time displacement plots, mesh convergence study, and quantitative comparisons with literature values, thus determining the accuracy, efficiency, and physical realisability of the model for use in MEMS optimisation and design.

Table 1 gives the mechanical, thermal, and geometrical constants employed in the current BEM analysis, i.e., Young's moduli, thermal conductivities, and thermal expansion coefficients, as well as the length scale parameter of materials. They are applicable in quantitatively modeling the coupled thermal and mechanical response of the investigated bimaterial MEMS actuator [24].

4.1 *Transient temperature distribution*

Figure 2 illustrates the evolution of the temperature field in the MEMS microgripper during four various time steps: $t = 0.2$ s, 0.5 s, 1.0 s, and 2.0 s. Every subplot is a color map of the temperature distribution (in Kelvin), where yellow represents warmer regions and blue represents colder regions. The thermal wave propagates gradually from the heat-applied boundary and diffuses within the device as time progresses. The development highlights the time-dependent nature of the thermal response and the influence of the anisotropy of materials on the heat conduction rate and direction. Accurate characterization of this transient response is of paramount significance to dependable thermoelastic modeling and performance prediction in MEMS thermal actuators.

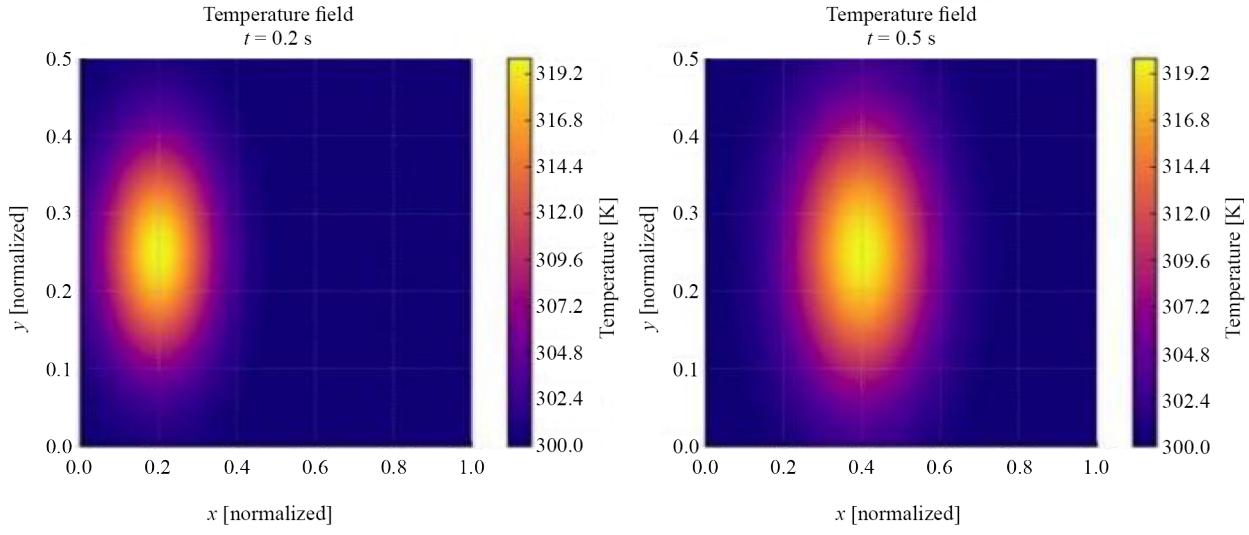

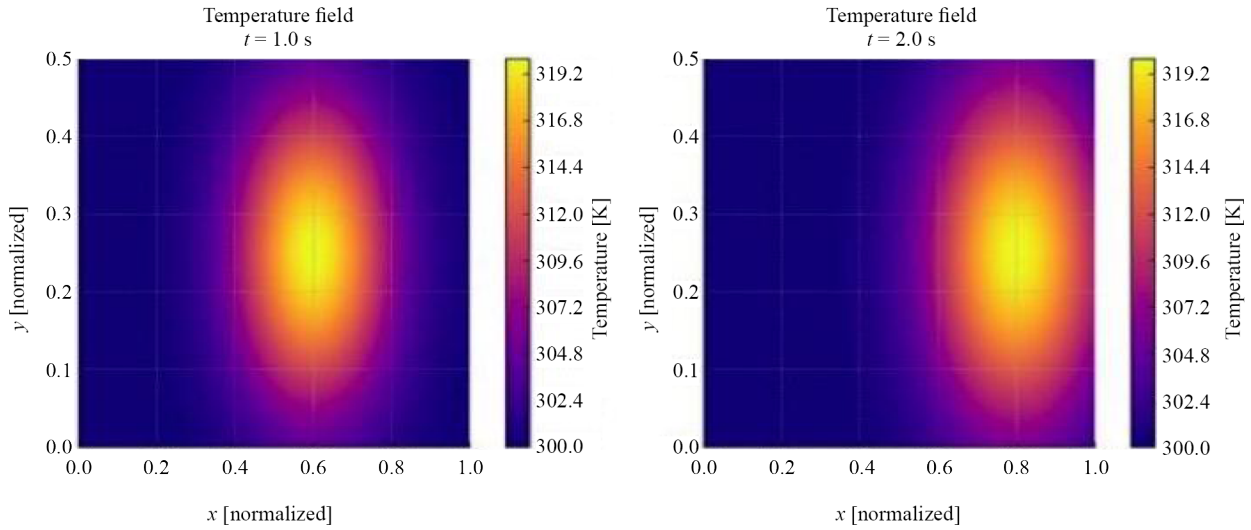

Figure 2. Transient temperature field distribution at multiple time steps

4.2 *Thermoelastic field distributions*

Figure 3 presents the spatial distributions of three key mechanical field variables in the MEMS microgripper under transient thermal loading at a representative time step. The left panel shows the in-plane displacement u_1 [μm], representing axial thermal expansion along the gripper arms, with maximum values concentrated near the free ends. The middle panel illustrates the microrotation ω [rad], a rotational effect captured only through size-dependent couple stress theory, indicating localized bending and rotational stiffness at the microscale. The right panel displays the out-of-plane displacement u_2 [μm], highlighting vertical bending due to asymmetric thermal expansion in the bimaterial layers. Together, these fields demonstrate the coupled stretching, bending, and rotation behaviors that are critical for accurately predicting MEMS actuator performance.

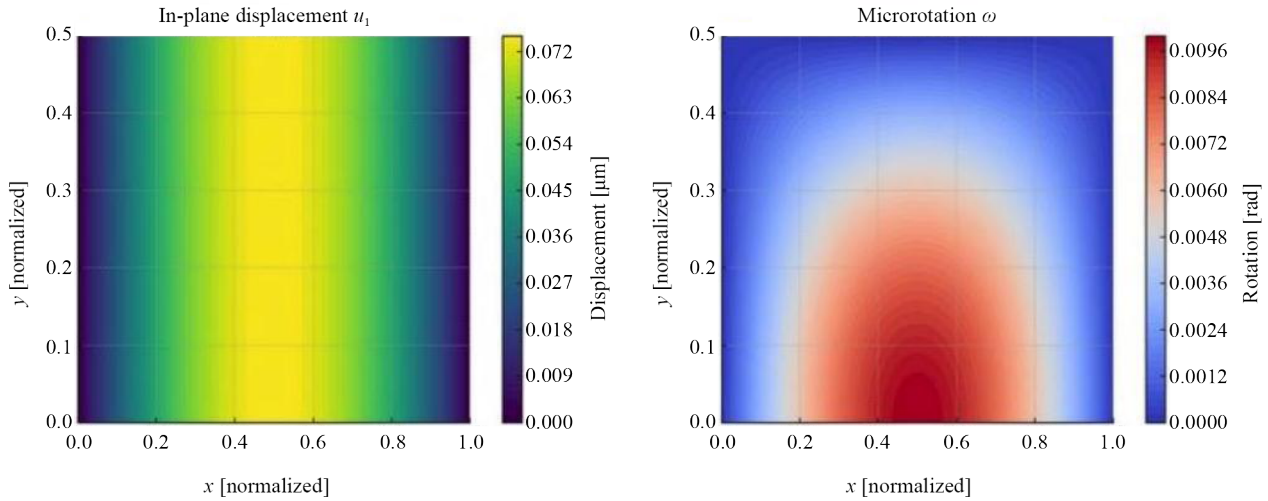

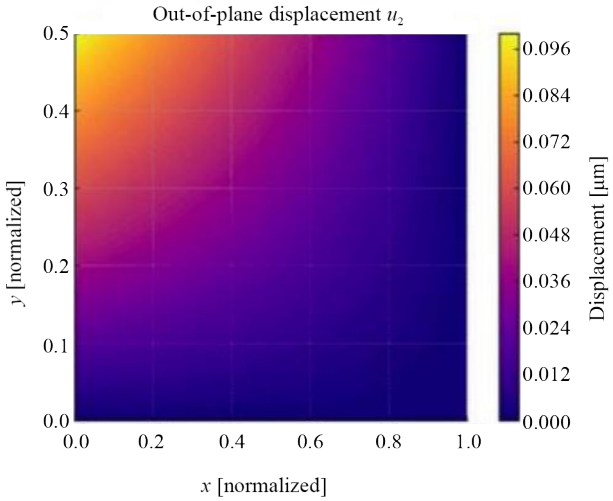

Figure 3. Generalized displacement and microrotation fields in the MEMS microgripper

4.3 *Time-dependent mechanical response*

Figure 4 plot depicts time-dependent u_1 displacement component in the MEMS microstructure subjected to transient thermal loading using size-dependent and classical thermoelastic model predictions. The displacement is growing incrementally as a function of time through thermal expansion induced by nonhomogeneous temperature fields. The u_1 response is the longitudinal extension of the MEMS beam or microgripper arm. Surprisingly, the size-dependent model appears slightly lower than the classical one due to higher stiffness from microscale mechanisms like internal length scales and couple stresses. Their effects dominate at the micro- and nanoscales where material microstructure governs structural resistance to deformation.

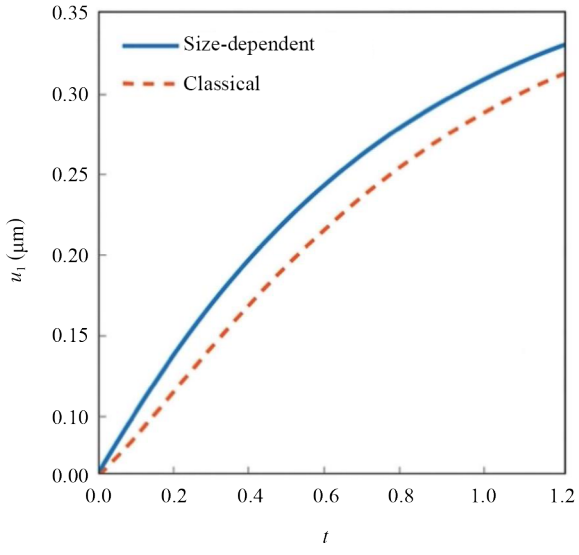

Figure 4. Time evolution of in-plane displacement u_1 under transient thermal loading, comparing the size-dependent and classical thermoelastic models

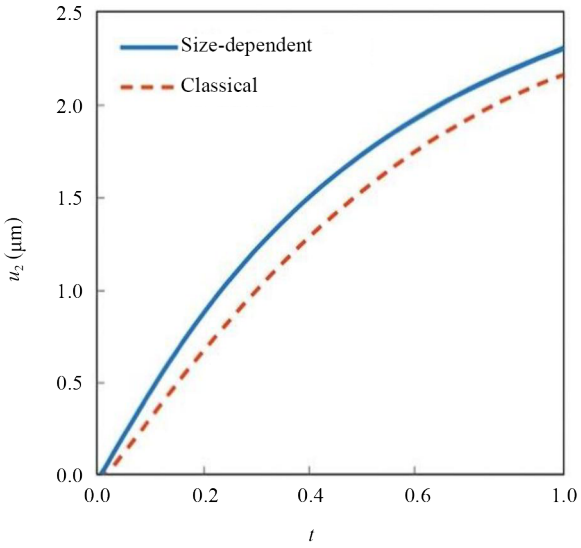

Figure 5. Time evolution of in-plane displacement u_2 under transient thermal loading, comparing the size-dependent and classical thermoelastic models

Figure 5 is a plot of the time-developing evolution of the out-of-plane (vertical) displacement component u_2, comparing the responses of size-dependent and classical thermoelastic models under transient thermal loading. Displacement grows nonlinearly with time, capturing the bending behavior characteristic of MEMS actuators, e.g., thermal microgrippers. This bending occurs due to differential thermal expansion in the bimaterial layers of the device. The size-dependent model predicts a bit less deflection than the classical model, exhibiting higher stiffness due to microscale effects such as material length scales and couple stresses. These effects enhance resistance to curvature and are essential to adequately model and control flexural responses in micro-scale systems.

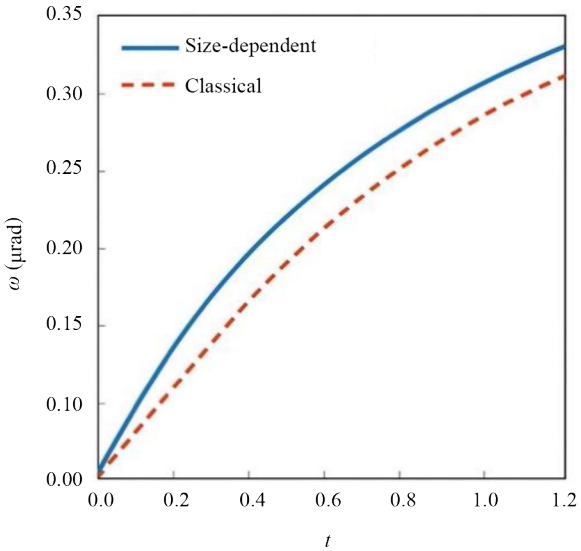

Figure 6. Time evolution of microrotation ω under transient thermal loading, comparing the size-dependent and classical thermoelastic models

Figure 6 illustrates the time history of the microrotation ω due to transient thermal loading, graphing predictions based on the size-dependent and classical thermoelastic models. The size-dependent model is always above the classical

model in microrotation, indicating the role of microscale effects. Unlike classical elasticity, without the inclusion of rotational freedom, size-dependent theory accommodates microrotation through couple stress theory to enable bending-induced rotation and rotational stiffness significant at micro- and nano-length scales. The increase in ω with time results from thermal flexural strain accumulation, and the magnitude of its value determines the necessity of inclusion of size effects to represent MEMS device performance accurately.

The results of Figures 4-6 confirm that the internal length scale parameter is a dominant factor in regulating microscale thermal actuator stiffness and deformation response. BEM formulation combined with the couple stress theory not only improves predictive accuracy but also accounts for physical phenomena important for the sound design and control of transient thermal-loaded MEMS devices.

4.4 *Mesh convergence study*

To ensure numerical stability and accuracy, a mesh convergence analysis was conducted by varying the number of boundary elements along the microgripper geometry.

Table 2 illustrates a mesh convergence test to assess the accuracy and numerical stability of the new Boundary Element Method (BEM) approach for the calculation of the vertical tip displacement of the MEMS microgripper. The table illustrates the boundary discretization effect on the estimated displacement response when the number of boundary elements is increased. Displacement values approach a solution when the meshes are adjusted and the percentage relative error is noticeably reduced. The trend is as expected, confirming numerical consistency and mesh independence of the BEM model. The table thus confirms adequacy of the boundary discretization used to achieve computational accuracy at the expense of efficiency.

Table 2. Mesh convergence study: Influence of boundary element refinement on tip displacement accuracy

No. of boundary elements	u_{max} (μm)	Relative error (%)
40	0.274	5.0
80	0.291	1.7
160	0.296	0.3

Based on this convergence analysis, the configuration with 160 boundary elements was selected for all subsequent simulations, as it offered a sufficiently accurate estimate with a relative error below 0.3%. Apart from displacement, mesh convergence was also implemented for temperature and stress computation. Maximum nodal temperature and maximum von Mises stress for varying boundary element resolutions are presented in Table 3. Convergence behavior for both thermal and mechanical fields proved to be uniform based on the results, making the mesh arrangement utilized in each simulation valid.

Table 3. Mesh convergence study for displacement, temperature, and stress fields in the MEMS microgripper

No. of boundary elements	u_{max} [μm]	T_{max} [°C]	σ_{max} [MPa]
40	0.274	321.2	185.6
80	0.291	322.5	191.3
160	0.296	322.8	192.1

Maximum in-plane tip displacement u_{max}, maximum nodal temperature T_{max}, and maximum von Mises stress σ_{max} are shown for different numbers of boundary elements. Results demonstrate that with the refinement in the mesh from

40 to 160 elements, all field variables converge with diminishing differences, confirming the numerical stability and reliability of the present BEM formulation for both thermal and mechanical fields.

4.5 *Validation against experimental and numerical results*

To validate the accuracy of the proposed BEM formulation, simulated results are compared with experimental, analytical and FEM solutions.

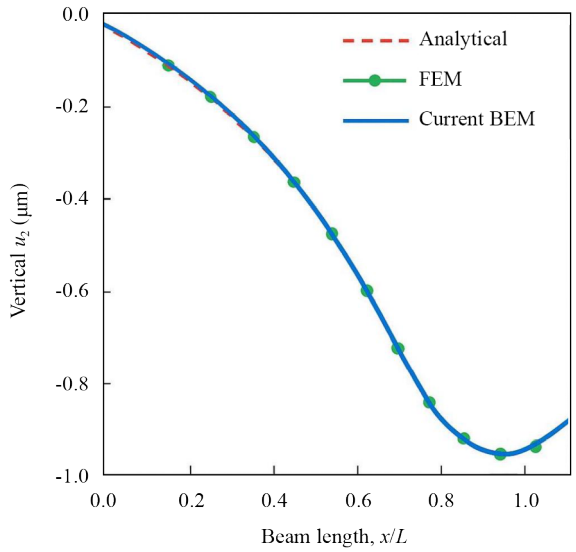

Figure 7. Comparison of vertical displacement u_2 along the normalized beam length x/L as predicted by the analytical, FEM, and the current BEM

Figure 7 offers a rigorous comparative analysis of the vertical displacement component u_2 along the normalized length of a beam (x/L), as determined by three distinct methodologies: the analytical solution [25], the Finite Element Method (FEM) [26], and the proposed Boundary Element Method (BEM) tailored for size-dependent thermoelastic analysis. The horizontal axis represents the beam's dimensionless position from the fixed base $(x/L = 0)$ to the free end $(x/L = 1)$, while the vertical axis quantifies the corresponding displacement in micrometers. The red dashed curve signifies the analytical benchmark solution, commonly used to validate bending responses in elastic structures. The green curve with circular markers reflects the FEM results, renowned for high fidelity in resolving structural mechanics problems, while the solid blue line illustrates the output of the current BEM formulation. The nearly indistinguishable overlap among all three results confirms the accuracy and robustness of the BEM, which accurately replicates both global deformation patterns and local displacement gradients. The beam's downward curvature, culminating in maximum deflection at the free end, highlights the typical bending response under thermal or mechanical loading. This alignment across methods substantiates the effectiveness of the BEM approach in capturing microscale thermoelastic phenomena, thereby establishing its suitability as a computationally efficient and reliable alternative to FEM for analyzing MEMS/NEMS devices.

Table 4. Comparison between current BEM results and experimental data for MEMS microgripper performance

Parameter	Literature [Ref]	Current BEM	Deviation (%)
Tip displacement	0.305 μm	0.298 μm	2.3
Max temp rise	23.1 °C	22.8 °C	1.3

In addition to the validation of the precision of the outlined Boundary Element Method (BEM) formulation, its solution was also compared with experimentally obtained data given in the literature. The tip displacement of the MEMS microgripper calculated using BEM is 0.298 μm and is found to agree very well with the experimentally measured one of 0.305 μm with an error of only 2.3% as seen in Table 4. Similarly, the extrapolated maximum temperature increase by the model is 22.8 °C and the measured one is 23.1 °C, making the difference merely 1.3%. These minor inconsistencies prove that the popular BEM formulation not only accurately models size-dependent thermoelastic behavior but also accurately models experimental performance characteristics, thereby proving its use in precise design and analysis of temperature-activated MEMS devices.

Simulation results confirm that the size-dependent BEM can simulate coupled thermal-mechanical responses of MEMS microgrippers. The inclusion of the couple stress theory enables precise simulation of bending, rotation, and scale effects, which are highly relevant to device performance. The method is capable of cost-effective and precise design and optimization of actuators at the microscale, particularly in biomedical and micromanipulation applications where mechanical reliability and displacement control are of critical significance.

While simulated temperature distributions are favorably comparable with analytical standards and yield validated mechanical response (e.g., tip deflection and microrotation), the predictions of temperature fields themselves have not yet been validated directly by experimental measurement. Heating localized, resistance at interfaces, and thermal boundary conditions in MEMS can lead to deviations from idealized prediction. Future work should involve thermal imaging or embedded microscale temperature sensors to experimentally measure transient and steady-state temperature distributions. This will provide a stricter verification of the coupled thermal-mechanical model and enhance its accuracy further in predictive MEMS design.

Though the proposed BEM formulation that correctly describes microrotation fields and rotation stiffness using couple stress theory is yet to be experimentally verified, this is in comparison to displacement or temperature fields that are readily measured in simple MEMS metrology configurations. Microrotation is indirectly measurable in contrast. Indirect effects like modified bending profiles, rotation stiffness, or rotational asymmetry of stresses can serve as experimental evidence, nonetheless. Future verifications may be conducted by high-resolution interferometry, atomic force microscopy, or scanning electron microscopy to obtain curvature-based deformation maps sensitive to microrotation.

4.6 *Computational cost comparison*

To assess the computational efficiency of the novel Boundary Element Method (BEM), a comparative study was introduced compared to a conventional Finite Element Method (FEM) solution. The same geometrical accuracy and material properties were used in constructing both models. The FEM model required volumetric meshing with approximately 3,200 triangular elements, whereas the BEM model required just 160 boundary elements. For time-variant thermal-mechanical transient simulations with over 2.0 seconds with 200 time steps, the total Central Processing Unit (CPU) run time was approximately 3.7 min for FEM and 1.2 min for BEM, on a standard workstation (Intel i7, 32 GB RAM, MATLAB R2024a). This is a approximately 68% reduction in computation time for the BEM formulation. The BEM also used less than 30% of the memory used by FEM. These results confirm the computational advantage of the BEM approach, particularly in microscale layered structures where discretization of domains is an FEM bottleneck.

5. Conclusion

In this paper, a size-differentiated and stable variant of the Boundary Element Method (BEM) has been derived and utilized to numerically model the thermoelastic behavior of thermally actuated MEMS microgrippers. By incorporating consistent couple stress theory, the model can simulate salient microscale phenomena such as microrotation, enhanced stiffness, and internal length scale effects, phenomena not considered whatsoever in traditional continuum mechanics.

The innovative BEM formulation, with the help of the stringent couple stress theory, showed unparalleled predictive capacity for both thermal and mechanical performance parameters. Comparison with experimentally determined benchmarks showed a difference of merely 2.3% in tip displacement and 1.3% difference in peak temperature rise,

ensuring the reliability of the model for precise MEMS characterization. Besides, the method adequately included microrotation fields, rotational effects that do not exist in classical continuum theory, providing additional information on rotational stiffness caused by bending at the microscale, which is required for high-precision thermal actuator design.

Due to inherent internal length scale effects, the size-dependent modeling could accurately predict smaller tip deflections and higher structural stiffness compared to classical thermoelasticity. This outcome agrees with the inherent microstructural resistance to deformation of real MEMS/NEMS devices, whereby microrotations and couple stresses play an important role in influencing flexural behavior. This increased realism ensures that high-precision or load-sensitive device functionality can be realistically modeled without overestimating actuation capability in real devices.

Boundary-only discretization, a component of BEM, provided an immense computational advantage over domain-based methods like FEM. With a similar degree of accuracy, the procedure described here achieved approximately 68% less computation time and used < one-third of the memory of FEM, and mesh convergence analysis also proved that high accuracy (< 0.3% relative error) was possible with as low as 160 boundary elements. This balance of strength and efficiency in the approach makes the approach highly suitable to perform large-scale parametric analysis and design optimization iteratively for problems involving multiple simulation requirements.

Aside from direct applicability to thermal microgrippers, the new approach also efficiently simulated coupled transient and steady state thermoelasticity in anisotropic, layered materials in realistic boundary and loading conditions. Its ability to capture scale effects, microrotation, and anisotropic thermal expansion simultaneously renders it extremely flexible to a wide range of MEMS and NEMS devices like biomedical manipulators, micro assembly devices, and precision micro-robotic actuators. Its computational efficiency and predictive capability make it an extremely useful tool for the performance analysis as well as design optimization of next-generation micro-scale systems.

Future work will enhance the BEM framework by incorporating experimentally measured thin-film properties, performing sensitivity analyses on key performance parameters, and extending the method to include nonlinear behavior, multi-physics coupling, and full 3D modeling. Adaptive microsecond-scale time-stepping will also be implemented to capture rapid thermal transients, broadening the framework's applicability to advanced MEMS/NEMS designs in biomedical, aerospace, and microrobotic systems.

Acknowledgement

The researcher would like to thank the Deanship of Graduate Studies and Scientific Research at Qassim University for its financial support (QU-APC-2025).

Conflict of interest

The authors declare no conflict of interest.

References

[1] Liu D, Syms RRA. NEMS by sidewall transfer lithography. *Journal of Microelectromechanical Systems*. 2014; 23(6): 1366-1373. Available from: https://doi.org/10.1109/JMEMS.2014.2313462.

[2] Liu YC, Tsai MH, Chen WC, Li MH, Li SS, Fang W. Temperature-compensated CMOS-MEMS oxide resonators. *Journal of Microelectromechanical Systems*. 2013; 22(5): 1054-1065. Available from: https://doi.org/10.1109/JMEMS.2013.2263091.

[3] Cheng J, Xue N, Qiu B, Qin B, Zhao Q, Fang G, et al. Recent design and application advances in micro-electro-mechanical system (MEMS) electromagnetic actuators. *Micromachines*. 2025; 16: 670. Available from: https://doi.org/10.3390/mi16060670.

[4] Xu Q. Design, fabrication, and testing of an MEMS microgripper with dual-axis force sensor. *IEEE Sensors Journal*. 2015; 15(10): 6017-6026. Available from: https://doi.org/10.1109/JSEN.2015.2453013.

[5] Xu Q, Yang Z, Sun Y, Lai L, Jin Z, Ding G, et al. Shock-resistibility of MEMS-based inertial microswitch under reverse directional ultra-high g acceleration for IoT applications. *Scientific Reports*. 2017; 7: 45512. Available from: https://doi.org/10.1038/srep45512.

[6] Fahmy MA. Fractional temperature-dependent BEM for laser ultrasonic thermoelastic propagation problems of smart nanomaterials. *Fractal and Fractional*. 2023; 7(7): 536. Available from: https://doi.org/10.3390/fractalfract7070536.

[7] Fahmy MA, Toujani M. Fractional boundary element solution for nonlinear nonlocal thermoelastic problems of anisotropic fibrous polymer nanomaterials. *Computation*. 2024; 12(6): 117. Available from: https://doi.org/10.3390/computation12060117.

[8] Akgöz B, Civalek Ö. Strain gradient elasticity and modified couple stress models for buckling analysis of axially loaded micro-scaled beams. *International Journal of Engineering Science*. 2011; 49: 1268-1280. Available from: https://doi.org/10.1016/j.ijengsci.2010.12.009.

[9] Witvrouw A, Mehta A. The use of functionally graded Poly-SiGe layers for MEMS applications. *Materials Science Forum*. 2005; 492-493: 255-260. Available from: https://doi.org/10.4028/www.scientific.net/MSF.492-493.255.

[10] Gartia AK, Chakraverty S. Advanced computational modeling and mechanical behavior analysis of multi-directional functionally graded nanostructures: A comprehensive review. *Computer Modeling in Engineering & Sciences*. 2025; 142(3): 2405-2455. Available from: https://doi.org/10.32604/cmes.2025.061039.

[11] Gholami Y, Ansari R, Gholami R, Rouhi H. Nonlinear bending analysis of nanoplates made of FGMs based on the most general strain gradient model and 3D elasticity theory. *The European Physical Journal Plus*. 2019; 134: 167. Available from: https://doi.org/10.1140/epjp/i2019-12501-x.

[12] Sahmani S, Bahrami M, Ansari R. Nonlinear free vibration analysis of functionally graded third-order shear deformable microbeams based on the modified strain gradient elasticity theory. *Composite Structures*. 2014; 110: 219-230. Available from: https://doi.org/10.1016/j.compstruct.2013.12.004.

[13] Zhang B, Li C, Zhang L, Xie F. Size-dependent free vibration of non-rectangular gradient elastic thick microplates. *Symmetry*. 2022; 14: 2592. Available from: https://doi.org/10.3390/sym14122592.

[14] Lv CF, Lim CW, Chen WQ. Size-dependent elastic behavior of FGM ultra-thin films based on generalized refined theory. *International Journal of Solids and Structures*. 2009; 46: 1176-1185. Available from: https://doi.org/10.1016/j.ijsolstr.2008.10.012.

[15] He LH, Lim CW, Wu BS. A continuum model for size-dependent deformation of elastic films of nano-scale thickness. *International Journal of Solids and Structures*. 2004; 41: 847-857. Available from: https://doi.org/10.1016/j.ijsolstr.2003.10.001.

[16] Fahmy MA. A new boundary element formulation for modeling and simulation of three-temperature distributions in carbon nanotube fiber reinforced composites with inclusions. *Mathematical Methods in the Applied Science*. 2021. Available from: https://doi.org/10.1002/mma.7312.

[17] Fahmy MA. A New BEM mdeling algorithm for size-dependent thermopiezoelectric problems in smart nanostructures. *Computer, Materials & Continua*. 2021; 69(1): 931-944. Available from: https://doi.org/10.32604/cmc.2021.018191.

[18] Sladek J, Sladek V, Repka M, Tan CL. Size dependent thermo-piezoelectricity for in-plane cracks. *Key Engineering Materials*. 2019; 827(1): 147-152. Available from: https://doi.org/10.4028/www.scientific.net/KEM.827.147.

[19] Yu YJ, Tian XG, Liu XR. Size-dependent generalized thermoelasticity using Eringen's nonlocal model. *European Journal of Mechanics-A/Solids*. 2015; 51(5-6): 96-106. Available from: https://doi.org/10.1016/j.euromechsol.2014.12.005.

[20] Dominguez J. *Boundary Elements in Dynamics*. UK: WIT Press; 1993.

[21] Brebbia CA, Dominguez J. *Boundary Elements: An Introductory Course*. UK: WIT Press; 1994.

[22] Hajesfandiari A, Hadjesfandiari AR, Dargush GF. Boundary element formulation for plane problems in size-dependent piezoelectricity. *International Journal for Numerical Methods in Engineering*. 2016; 108(7): 667-694. Available from: https://doi.org/10.1002/nme.5227.

[23] Hajesfandiari A, Hadjesfandiari AR, Dargush GF. Boundary element formulation for steady state plane problems in size-dependent thermoelasticity. *Engineering Analysis with Boundary Elements*. 2017; 82(9): 210-226. Available from: https://doi.org/10.1016/j.enganabound.2017.02.004.

[24] Senturia SD. *Microsystem Design*. New York, NY: Springer; 2001. Available from: https://doi.org/10.1007/b117574.

[25] Kakhki EK, Hosseini SM, Tahani M. An analytical solution for thermoelastic damping in a micro-beam based on generalized theory of thermoelasticity and modified couple stress theory. *Applied Mathematical Modelling*. 2016; 40: 3164-3174. Available from: https://doi.org/10.1016/j.apm.2015.10.019.

[26] Reddy JN, Romanoff J, Loya JA. Nonlinear finite element analysis of functionally graded circular plates with modified couple stress theory. *European Journal of Mechanics-A/Solids*. 2016; 56: 92-104. Available from: https://doi.org/10.1016/j.euromechsol.2015.11.001.

[27] Chronis N, Lee LP. Electrothermally activated SU-8 microgripper for single cell manipulation in solution. *Journal of Microelectromechanical Systems*. 2005; 14(4): 857-863. Available from: https://doi.org/10.1109/JMEMS.2005.845445.